

3-20-92  
E6817

NASA Technical Memorandum 105412

# Collapse Analysis of a Waffle Plate Strongback for Space Station Freedom

Frank F. Monasa  
*Michigan Technological University*  
*Houghton, Michigan*

and

Joseph M. Roche  
*Lewis Research Center*  
*Cleveland, Ohio*

March 1992



# COLLAPSE ANALYSIS OF A WAFFLE PLATE STRONGBACK FOR SPACE STATION FREEDOM

Frank F. Monasa<sup>\*</sup>  
Michigan Technological University  
Civil and Environmental Department  
Houghton, Michigan 49931

and

Joseph M. Roche  
National Aeronautics and Space Administration  
Lewis Research Center  
Cleveland, Ohio 44135

## SUMMARY

The purpose of this study was to determine the structural integrity of the Integrated Equipment Assembly (IEA) Strongback of the Space Station Freedom for the launch environment. The strongback structure supports the electrical power system for Space Station Freedom. To achieve minimum launch mass, it is essential that flight structures, such as the strongback, are designed as light as possible. Therefore, the structural analyst must assure the structural integrity of the design. Consequently, a nonlinear structural analysis was conducted to determine the collapse load of the structure and the associated factor of safety against the service loads. Future analysis of flight structures having the general characteristics of the strongback may follow the methodology developed in this report. The report provides a modeling technique for simulating the load conditions and evaluation of the buckling and post-buckling (collapse) loads of the IEA Strongback structure, using the finite element computer code MARC (ref. 1). The MARC program was selected for this study due to its capability to perform collapse and nonlinear structural analyses. The strongback structure supports the electrical power system for Space Station Freedom. Two of four strongback panels were modeled and analyzed. This study dealt with the effect of the following factors on the global behavior of the strongback panels: (1) load simplification and simulation; (2) type of support boundary conditions; (3) the possibility of weight reduction of the original structure. For this purpose several models of the two panels of the strongback were considered. The stress level and distribution in the panels for the launch condition, the Eigenvalue critical buckling load and/or the collapse load were determined. Nonlinear structural analysis was required to determine the collapse load. Both geometrical nonlinearity (large deflections) and material nonlinearity were considered. It is shown that a weight reduction of the strongback panels is possible, while maintaining a reasonable factor of safety against the collapse load. This methodology may be useful for future analysis of similar structures.

## INTRODUCTION

The National Aeronautics and Space Administration is currently in the developmental phase of Space Station Freedom. The Space Station Freedom development task has been

---

<sup>\*</sup>Summer Faculty Fellow at NASA Lewis Research Center.

divided into four work packages. The Lewis Research Center has been delegated the responsibility for the development of the electrical power generation module for Space Station Freedom. A photovoltaic power generation system has been selected as the primary method of power generation. Several power generation subsystems are required. A power storage system of batteries is required to maintain the electrical power supply while the Space Station is in an eclipse period. In addition to the batteries, a significant amount of hardware is required for the power distribution and management system. A sun tracking and pointing system must be used to keep the photovoltaic arrays pointed towards the sun. The process of recharging the batteries generates a significant amount of waste heat, which must be rejected through a thermal control system. The Integrated Equipment Assembly (IEA) provides the structural framework (fig. 1) for the power generation subsystems. The IEA structural framework provides an interface for the power generation subsystems and the primary attachment to the orbiter cargo bay attachment points, during the shuttle launch. The three primary components of the IEA are the Keel bulkhead, the Longerons bulkhead and the Strongback. During the orbital operation, the IEA is a part of the primary structure for Space Station Freedom.

The objective of this research was to determine the stress level and distribution in the IEA Strongback under launch loading condition. In addition, the critical buckling load and the ultimate load carrying capacity (collapse load) were required to determine the safety factor in the IEA Strongback against buckling and collapse.

To perform the structural analysis of the IEA Strongback, an appropriate finite element code was required. Several finite element codes are available for the determination of stresses under launch loading conditions where linear structural analysis is adequate. However, to determine the buckling or the ultimate load carrying capacity of any structural system, a code capable of performing nonlinear structural analysis should be selected. The MARC program (ref. 1) was selected due to its ability to perform nonlinear structural analysis where both material and geometrical nonlinearities (large displacements) are considered, and to determine the collapse load. The availability of the BUCKLE, LARGE DISPLACEMENT, UPDATE, WORK HARD, and AUTO INCREMENT options in the nonlinear analysis portion of the program facilitated the determination of the collapse load and the corresponding deflections.

The structural system of the IEA Strongback is complex and it is subjected to complicated loading conditions. Due to the geometrical symmetry of the IEA Strongback, only half of the structure was considered, i.e., the two panels of the strongback were modeled without the longeron and keel bulkheads attachments. The model of two panels of the strongback were prepared using the preprocessor PATRAN (ref. 2). In order to properly interpret the results of the structural analysis of the finite element model using the MARC program, it was necessary to consider a simple loading condition to determine the compatibility between the two codes, PATRAN and MARC. This will be discussed in the next section. After a confidence in the stress interpretation was obtained, several models of the strongback panels were used to determine the stresses under loading condition that simulates launch environment. Several models were developed to determine the following affects:

1. The ORU (Orbital Replacement Units) loads simulation
2. The support boundary conditions
3. Diagonal stiffener effects on the strongback panels
4. Weight reduction of the strongback panels

The description of these models and their analysis results will be discussed in a later section of the report.

### The Physical Description and the Finite Element Models

The strongback panels consist of waffle construction (including orthogonal and diagonal stiffeners) with an overall width of 157.0 in., length of 142.46 in. and overall depth of 10 in. Aluminum alloy 6061-T651X was selected for the material of the strongback. Stress-strain relationships were based on material properties from MIL-HDBK-5E. Due to the symmetrical configuration of the strongback, it was possible to model half of the strongback structure. The finite element model was generated for MARC using PATRAN to process the geometric data. Figure 2 shows the geometrical configuration of one panel of the strongback. The two panels are connected by bolts. These joints are simulated by using the MARC tying option. A coarse finite element mesh was used in this study in order to be able to interpret the analysis results and the structural behavior of the strongback under its loading conditions, and to reduce the computer time needed to solve the problem. The finite element models of the strongback lower and upper panels are shown in figures 3 to 6. The node and element identification numbers are shown on the model. A total of 144 of the MARC type 75 elements were used. The type 75 element is a four-node thick shell element which supports the large displacement option in MARC. The file was edited so that the data is compatible with the input data requirements of the MARC program.

When the PATRAN preprocessor is used to construct the model, one must make sure that the node connectivity for all elements is in a counterclockwise direction. The direction of the element nodes connectivity affects the manner in which the uniform pressure and the traction forces act on the element. For example, load type 2 (uniform pressure on the surface) for element type 75 in the MARC program is positive in the direction of the negative  $V^3$  axis where the nodes connectivity is counterclockwise, as shown in figure 7. Therefore, the type of the element nodes connectivity affects the direction of the applied load.

### Loading Conditions

The flight loads imposed by the ORU boxes mounted to the upper and lower surface of the strongback were the only loads considered in this study. Several types of ORU boxes are mounted on the IEA. The heaviest, the battery ORU, will be assumed to populate the entire IEA. The weight of each battery ORU was conservatively assumed to be 400 lb. The base dimensions for each unit are 40 by 40 in. The ORU loads were assumed to be uniformly distributed on the strongback. The simplifying assumptions eliminate the structural interaction between the ORU and the structure. Concentrated forces at the attachment points are not considered. The ORU masses exert inertial forces (G load) onto the strongback structure during launch. The inertia forces specified for Cargo Element during the shuttle launch environment are -3.2 G, -1.4 G, and 2.5 G in the direction of the X, Y, and Z-axes, respectively.

The ORU loads were simulated as a uniform pressure (force/unit area) in the Z direction on the upper and lower panels of the strongback, and uniform traction loads (force/unit length) on the edges of each finite element in X and Y-axes directions. In addition, moments were applied about the X and Y-axes due to the position of the ORU's center of gravity. The following shows the determination of the uniform traction loads in the direction of the X and Y-axes

and the uniform pressure in the direction of the Z-axis, and the moments about the X and Y axes on the strongback surface.

1. Traction load in the X-axis direction

This is a uniform load which acts perpendicularly along the edges parallel to the Y-axis direction, and is measured in lb/in.

A finite element model of the upper panel of the strongback showing the element and node numbers is given in figure 8. To specify the traction loads on each finite element using the MARC program, it is important to specify the proper node connectivity for the element. In this model, the connectivity is considered to be in the counterclockwise direction, i.e., element number 73 connectivity nodes are 99, 97, 93, and 91. Therefore, the traction loads in the X and Y-axes directions on this element are shown in figure 9 as types 21 and 41, 11 and 31, respectively. The MARC program specifies that loading types 21 and 31 are in compression, therefore, they are considered to be positive, while loading types 11 and 41 are in tension, therefore, they are considered to be negative. The total traction load in the X-axis direction on each panel of the strongback is equal to:

$$\frac{142.46 \text{ in.} \times 78.50 \text{ in.}}{40 \text{ in.} \times 40 \text{ in.}} \times (400 \text{ lb}) \times 3.2 = 8946 \text{ lb}$$

This load is assumed to be distributed uniformly (lb/in.) along the edges of the four finite elements along the X-axis. Therefore, the load acting on these edges is equal to:

$$\frac{8946 \text{ lb}}{78.5 \text{ in.} \times 8} = 14.25 \text{ lb/in.}$$

This load is shown in figure 9 as load types 21 and 41.

2. Traction load in the Y-axis direction.

This is a uniform load which acts perpendicularly along the edges parallel to the X-axis direction, and is measured in lb/in.

The total traction load in the Y-axis direction on each panel of the strongback is equal to:

$$\frac{142.46 \text{ in.} \times 78.5 \text{ in.}}{40 \text{ in.} \times 40 \text{ in.}} \times 400 \text{ lb} \times 1.4 = 3914 \text{ lb}$$

This load is assumed to be distributed uniformly (lb/in.) along the edges of the four finite elements along the Y-axis. Therefore, the load acting on these edges is equal to:

$$\frac{3914 \text{ lb}}{142.46 \text{ in.} \times 8} = 3.434 \text{ lb/in.}$$

This load is shown in figure 9 as load types 11 and 31.

3. Pressure load in the Z-axis direction.

This load is a uniform pressure (measured in lb/in.<sup>2</sup>) and acts perpendicularly to the surface of the strongback panels, i.e., it is in the Z-axis direction. It is designated as type 2 load in the MARC program. It is determined as follows:

$$\frac{400 \text{ lb(ORU's weight/box)}}{40 \text{ in.} \times 40 \text{ in.}} \times 2.5 = 0.625 \text{ psi}$$

The total applied load for the two panels of the strongback is:

$$0.625 \times 142.46 \times 78.50 \times 2 = 13 \text{ 979 lb}$$

4. Moment about the X and Y-axes.

In addition to the traction loads in the X and Y-axes directions, and a pressure load in the Z-axis direction, uniform moments about the X and Y-axes will be exerted by the ORU on the strongback structure. The center of gravity of the ORU is assumed to be 10 in. from the surface of the strongback structure (i.e., the XY plane).

The traction loads in the X and Y-axes directions,  $P_x$  and  $P_y$  are equal to 14.25 lb/in. and 3.434 lb/in., respectively. These loads act at the ORU's center of gravity (c.g.). Figures 10 and 11 show the forces  $P_x$  and  $P_y$  at the ORU's c.g. and the equivalence of these forces at the surfaces of the upper and lower panels of the strongback, i.e., the forces  $P_x$  and  $P_y$ , the moment  $M_y = P_x d$ , and  $M_x = P_y d$ .

a. Moment  $M_y$

The traction force  $P_x$  is equal to 14.25 lb/in. The moment  $M_y$  induced by the traction forces will be assumed acting as point loads along the width of the strongback panels. The surface of the strongback is divided into 16 elements, 4 elements on each side. Therefore, the point moments acting at the intermediate nodes can be obtained as follows:

$$14.25 \text{ lb/in.} \left( \frac{78.5 \text{ in.}}{4} \right) 10 \text{ in.} = 2797 \text{ lb-in.}$$

(2800 lb-in. were used in the input data), and the point moments acting at the external nodes, therefore, are:

$$\frac{2800 \text{ lb/in.}}{2} = 1400 \text{ lb-in.}$$

These point moments will be used as input data in the POINT LOAD option, and they are given below for the lower panel as:

#### POINT LOAD

```

,,,1400.0,
2,26,10,49,
,,,2800.0,
4,5,7,12,17,21,25,33,38,41,45,47,
,,,5600.0,
13,28,35,16,19,29,31,40,43

```

Moments  $M_y$  applied at the nodal points for the lower panel are positive (+) while moments  $M_y$  applied at nodal points for the upper panel are negative (-), as shown in figure 10.

#### b. Moment $M_x$

The traction force  $P_y$  is equal to 3.434 lb/in. The moment  $M_x$  induced by the traction forces will be assumed acting as point loads along the length of the strongback panel. The point moments acting at the intermediate nodes can be obtained as follows:

$$3.434 \text{ lb/in.} \left( \frac{142.46}{4} \right) 10 \text{ in.} = 1223 \text{ lb-in.}$$

(1224 lb-in. is used in the input data), and the point moments acting at the external nodes, therefore, are:

$$\frac{1224 \text{ lb-in.}}{2} = 612 \text{ lb-in.}$$

These point moments will be used as input data in the POINT LOAD option, and they are given below for the lower panel as:

#### POINT LOAD

```

,,, - 612.0,
2,10,26,49,
,,, - 1224.0,
4,5,7,12,17,21,25,33,38,41,45,47
,,, - 2448.0,
13,16,19,28,29,31,35,40,43,

```

Moments  $M_x$  applied at the nodal points for the lower panel are negative (-), while moments  $M_x$  applied at nodal points for the upper panel are positive (+), as shown in figure 11.

There will be no moments about any axis by transferring the load  $P_z$  from the ORU's center of gravity to the surface of the strongback panels.

## 5. Gravity Load

The application of gravity load (weight of the strongback) is achieved by using IBODY load type 102. The acceleration can be given independently in the X, Y, and Z directions through the DIST. LOADS option. In determining the weight, the mass density value must be given in the materials property card.

## MODEL DESCRIPTIONS

This study includes 10 models of the IEA Strongback panels. These models are described in appendix I. Also, schematic diagrams for the back-to-back panels of the strongback are shown in table I. These models were altered to study the effect of the following factors on the overall structural response of the strongback panels: (1) loading conditions; (2) change in support boundary conditions; (3) thickness reduction of the panel surface and stiffeners; and (4) removal of the diagonal stiffeners.

## DISCUSSION OF RESULTS

In this study, it was possible to: (1) simulate the ORU's loads on the two panels of the strongback structure, (2) determine the stresses for the launch loading condition, and (3) determine the buckling load and/or the collapse load. Any other type of loads on the strongback may be simulated in the same manner. The structural interaction between the ORU and the strongback structure have not been considered in this study.

To simulate a uniform pressure, traction loads, point moments, and gravity load on the strongback structure, several models were considered. Some of the models used to study the effect of only one loading condition. The model was increased in complexity as confidence was obtained in the simulation procedure of the previous models.

Table I shows the models used in this study, their support boundary conditions, the depth of each panel of the strongback, type of loading for each model, and analysis results. Model STG1 represents the original strongback panels. The preprocessor in PATRAN was used to construct the model. Due to the interface of PATRAN and MARC, the element nodes connectivity for the lower panel of the strongback was in a clockwise direction. To maintain compatibility with MARC, the element nodes connectivity was changed in model STG2A, to a counterclockwise direction and the loading was considered to be in the +Z direction only. This simple loading condition assured the accuracy of the uniform load simulation and provided an equilibrium check for the applied forces and the support reactions. The stresses for this model were post-processed using PATRAN. The stress distribution in the X and Y directions, and the nodal and element Von Mises stresses for the upper and the lower panels of the strongback in model STG2A are shown in figures 12 to 15, and in figures 16 to 19, respectively. There was a good

correlation between the stress diagrams from PATRAN and MARC output for all stresses except the element Von Mises stresses. The MARC output shows that the stresses (including Von Mises) and the displacements matched the results for the corresponding elements. Whereas, the element Von Mises stresses post-processed by PATRAN did not show this agreement. It was determined that the reason for this variation is that the elements Von Mises stresses in MARC are computed at the Gaussian points. The Gaussian points and the nodes for element type 75 are shown in figure 7.

To verify the analysis from MARC, the strongback model of STG2A was analyzed using NASTRAN (ref. 3). The stress values obtained from both codes were very close. Figures 20 and 21 show the stress distribution in the X axis direction and the Von Mises stresses in the upper panel of the strongback. These diagrams were prepared using the stress values obtained from NASTRAN and the post-processor from IDEAS (ref. 4).

The strongback structure in model STG3 was subjected to traction forces and gravity loads, due to the weight of the strongback, in addition to the uniform pressure on the surface of the strongback. This model was used to ensure the simulation of the traction and gravity forces and to check the equilibrium of the applied forces and the support reactions.

The Eigenvalue critical buckling load for the strongback structure is determined using model STG3B5. The linear buckling load is determined to be 966.7 times the current load on the structure, and the weight of the two panels of the strongback is 690.3 lb. It is shown that the 5 in. panels deep of the strongback have a large buckling load, therefore, the depth of each panel was reduced from 5 to 2 in., as shown in model STG3B2 in table I. The linear buckling load was 174.3 times the current load and the weight was reduced to 473.4 lb as found in table I. This amounts to an 82 percent reduction in the buckling load and a 31 percent reduction in the weight of the strongback in model STG3B5.

To reduce the weight of the strongback, the thickness of the panel skin was changed from 0.15 to 0.10 in., thickness of the end stiffeners was reduced from 0.5 to 0.25 in., and the remaining stiffeners were considered to have a thickness of 0.15 in. All other properties of model STG3B2 were retained. This model is given in STG4B2. The buckling load was 123.8 times the current load and the weight was reduced to 328.6 lb. This amounts to an 87 percent reduction in the buckling load and a 52 percent reduction in the weight of the strongback in model STG3B5.

To determine the effect of the support boundary conditions, the upper panel's supports were removed as shown for model STG4B2P in table I. The critical buckling load was 43.3 times the current load. This shows that the support boundary conditions have a large effect on the value of the buckling load.

To determine the effect of the removal of the diagonal stiffeners, model STG5B was prepared. The linear buckling load was 40.3 times the current load and the weight was reduced to 270.8 lb. Comparing models STG5B with STG4B2P, it is shown that there is a 7 percent reduction in the buckling load while the weight reduction in the panels amounts to 18 percent. The removal of the diagonal stiffeners has a little effect on the buckling load, while it has a larger effect on reducing the weight of the panels. It was shown also that the nodal displacements in model STG5B were large relative to the thickness of the skin of the panel. Therefore, this model was modified in order to include the effect of large deflection on the collapse load (see model STG5BL). A nonlinear analysis was required. Two options in MARC were used, i.e., LARGE

DISP (large displacements) and LOAD COR (residual load correction). The collapse load was determined to be 2.593 times the current load. In this analysis, the collapse load was determined in one step. However, MARC provides other options in the nonlinear analysis to provide a better representation of the collapse load. In addition to the LARGE DISP and LOAD COR options, MARC provides options for UPDATE (updating the coordinates), AUTO INCREMENT, and WORK HARD. All these options were used in the construction of model STG6L. The AUTO INCREMENT option allows the determination of the collapse load in a step-by-step manner. In this model the collapse load is specified to reach its value in 10 increments. The initial load of 10 percent of the final load is assumed to increase automatically up to the collapse load. The option WORK HARD allows tracing the actual stress-strain diagram of the material. The moment forces, induced by the ORU's during launch loading condition, had a negligible effect on the collapse load of the strongback panels. The collapse load for the model of STG6L was determined to be 6.4 times the current load. Figures 22, 23, and 24 show the maximum and minimum stress distribution, and the element Von Mises stresses, respectively, for the upper panel of the strongback.

### CONCLUDING REMARKS

In this study the stresses for a launch loading condition, the buckling load and/or the collapse loads were determined for the two panels of the IEA Strongback. It was determined that a weight reduction of the original configuration of the strongback structure and removal of the diagonal stiffeners is possible. The margin of safety relative to the collapse load is reasonable. It is about 6.4 times the load for launch conditions.

The ORU, utility plates, battery boxes, BCDU's, DCSU's, and other units do not exert just uniformly distributed loads on the strongback. Most of the units are anchored to the strongback at specified locations. Therefore, the effect of these units attachment type to the strongback should be taken into consideration when simulating the loads. The structural interaction of the ORU's with the skin of the strongback must be considered in the load simulation.

The significance of the report is to address and document the procedure used to conduct a nonlinear analysis of the strongback panels where both geometrical and material nonlinearities are considered. This report documents in details the application of the MARC program to simulate the launch loading condition and the determination of the collapse load of the strongback panels. The methodology can be used for other type of structures where a nonlinear analysis and the determination of the collapse load is required. It is shown that the pre and post-processor of PATRAN should be used with care in developing the finite element model, and plotting the stress distribution.

Further checks to investigate the natural frequency of the modified strongback structure must be performed to verify its compatibility with the space shuttle cargo element dynamics requirements.

APPENDIX I.  
BRIEF DESCRIPTION OF THE MODELS

## STG1.DAT

<b>Title:</b>	Linear Analysis of the Strongback Panels
<b>Connectivity:</b>	The PATRAN preprocessor is used to construct the model. When the input data is interfaced with MARC, the elements' nodes connectivity is considered to be in the clockwise direction for the lower panel and in the counterclockwise direction for the upper panel elements.
<b>Panel depth:</b>	5 in.
<b>Loading:</b>	Uniform pressure in the +Z-axis direction and uniform traction loads in the X and Y-axes directions.
<b>Support Conditions:</b>	<p>Left supports—restrained displacements and rotations in the X, Y, and Z directions for both panels.</p> <p>Right support—restrained displacements in the X, Y, and Z directions for both panels.</p> <p>A schematic diagram for the supports boundary conditions between the longeron and the keel bulkheads for both panels is shown in table I.</p>
<b>Tying:</b>	Type 100
<b>Print Option:</b>	Analysis results are printed for all elements.
<b><u>Note</u></b>	The element nodes connectivity for element type 75 in the MARC program is considered to be in a counterclockwise direction. The nodes connectivity for the elements in the lower panel of the strongback which they were translated using the PATRAN preprocessor is in a clockwise direction. Therefore, the lower panel nodes connectivity are changed in the next model so that the element nodes connectivity for both panels is in a counterclockwise direction.

## STG2A.DAT

**Title:** IEA Strongback Linear Structural Analysis of the Upper and Lower Panels

This model is similar to STG1.DAT except that:

- a. the applied load is a uniform pressure acting in the +Z-axis direction (type 2 in MARC),
- b. the nodes connectivity for the elements in the lower panel of the strongback are in a counterclockwise direction,
- c. tying type is Type 103 instead of Type 100, and
- d. stresses are printed for elements 1, 4, 6, 13, 16, 17, 73, 78, 85, and 89.

Note (refer to Vol. 3 of MARC Manual—Element Type 78)

Tying Type 103 ties the 3 degrees of freedoms (DOF) 1, 2, and 3, i.e., translations in the X, Y, and Z directions, however, tying Type 100 ties 6 degrees of freedom, i.e., translations and rotations in the X, Y, and Z directions. The usage of tying Type 103 instead of 100 has a very small effect on the magnitudes of stresses and deformations in the strongback panels. The structure is very stiff and it does not deflect enough to cause any appreciable changes in the stresses and displacements.

## STG3.DAT

**Title:** IEA Strongback Linear Structural Analysis—Upper and Lower Panels

This model is similar to STG2A.DAT except that the applied loads are a uniform pressure (psi) in the +Z-axis direction and traction uniform loads (lb/in.) in the -X, and -Y axes directions, plus gravity loads Type 102. The coefficients for the gravity load are -3.2, -1.4, and +2.5 in the X, Y, and Z directions, respectively.

## STG3B5.DAT

Note The letter B in the file name refers to the BUCKLE option and the number 5 refers to the depth of each panel.

**Title:** Determination of the Eigenvalue Linear Buckling Load for the IEA Strongback

This model is similar to STG3.DAT except that the supports condition was changed so the X translation DOF of the right supports is not restrained, as shown in the schematic diagram in table I.

### STG3B2.DAT

Note

The letter B in the file name refers to the BUCKLE option and 2 refers to the depth of each panel of the IEA Strongback.

**Title:**

Determination of Eigenvalue Linear Buckling Load

This model is identical to the model of STG3B5.DAT except that the overall depth of each panel of the strongback is 2 in. rather than 5 in. A schematic diagram for the model support boundary conditions and depth of each panel is shown in table I.

### STG4B2.DAT

**Title:**

Determination of Eigenvalue Linear Buckling Load

This model is similar to the model in STG3B2.DAT, except that the thickness of the panels skin is changed from 0.15 to 0.10 in., thickness of the end stiffeners is changed from 0.5 to 0.25 in., and the remaining stiffeners are considered to have a thickness of 0.15 in. All other properties of model STG3B2.DAT have been retained.

### STG4B2P.DAT

**Title:**

Determination of Eigenvalue Linear Buckling Load

This model is similar to the model in STG4B2.DAT, except that the boundary support conditions of the left supports of the lower panel of the IEA Strongback are now restrained for displacements in the X, Y, and Z-axes directions only, and the restraints for the upper panel have been removed. A schematic diagram for this supports boundary condition is shown in table I.

### STG5B.DAT

**Title:**

Determination of Eigenvalue Linear Buckling Load

This model is similar to the model in STG4B2P.DAT, except that all the diagonal stiffeners have been removed from the model.

### STG5BL.DAT

**Title:** Determination of the Nonlinear Buckling Load

This model is similar in geometry, loading, and support boundary conditions to the model in STG5B.DAT. In the previous models the Eigenvalue linear buckling loads were determined. To determine the nonlinear buckling load, two additional options in the MARC program are used, i.e., LARGE DISP (large displacement) and LOAD COR (residual load correction).

Note The letter L in the file name refers to large displacement option.

### STG6L.DAT

**Title:** Determination of Collapse (Ultimate Carrying Capacity) Load

This model is similar to the model in STG5BL.DAT, except that the moment forces induced by the ORU's during launch loading condition has been added to the loads in the previous models. In addition to the options used in STG5BL. DAT model, the UPDATE option was used to update the coordinate due to the large deflections effect, and the AUTO INCREMENT option is used to attain the collapse load in a step-by-step procedure rather than the BUCKLE option. Also, the WORK HARD option is added in order to consider the effect of material nonlinearity. The input data file for determining the collapse load for this model is given in appendix II.

APPENDIX II  
INPUT DATA FILE FOR MODEL  
STG6L.DAT

```

# USER=edas2 PW=asce12
# @$ -r stg61
# @$ -lT 120
# @$ -lt 115
# @$ -lM 1.9Mw
# @$ -eo
set -xk
cat >usub4.f <<"=EOF="
    SUBROUTINE ELEVAR (N,NN,LAYER,GSTRAN,GSTRES,STRESS,PSTRAN,
    1CSTRAN,VSTRAN,CAUCHY,EPLAS,EQUIVC,SWELL,KRTYP,PRANG,DT,
    2GSV,NGENS,NGEN1,NSTATS,NSTASS,THERM)
    COMMON/FAR/FACR,INC
    DIMENSION GSTRAN(NGENS),GSTRES(NGENS),
    1STRESS(NGEN1),PSTRAN(NGEN1),CSTRAN(NGEN1),VSTRAN(NGEN1),
    2CAUCHY(NGEN1),DT(NSTATS),GSV(1),THERM(NGENS)
C    OUTPUT OF MARC RESULTS
    I=INC
    TT=DT(1)
    SHY=(STRESS(1)+STRESS(2))/3.
    SX=STRESS(1)-SHY
    SY=STRESS(2)-SHY
    SZ=-SHY
    SIGE=SQRT((3./2.)*(SX**2+SY**2+SZ**2+2.*((STRESS(3))**2
    *+(STRESS(4))**2+(STRESS(5))**2)))
    EX=GSTRAN(1)
    EY=GSTRAN(2)
    EHY=(EX+EY)/3.
    EXH=EX-EHY
    EYH=EY-EHY
    EZH=-EHY
    EQTOT=SQRT((2./3.)*(EXH**2+EYH**2+EZH**2+.5*((GSTRAN(3))**2
    *+(GSTRAN(4))**2+(GSTRAN(5))**2)))
    ETEFF=EQTOT*1.0E6
C    IF(N.GT.2176) GO TO 62
    IF(NN.GT.1) GO TO 62
C    IF(INC.LT.20) GO TO 62
    IF(INC.EQ.0.AND.N.EQ.1) WRITE(41,61)
61    FORMAT(5H INC,5H ELEM,9H SIGE,10H SIG11,10H SIG22)
    WRITE(41,60) I,N,SIGE,STRESS(1),STRESS(2)
60    FORMAT(2I5,2X,F9.3,1X,F9.3,1X,F9.3)
62    CONTINUE
    RETURN
    END
    SUBROUTINE WKSLP(SLOPE,EBARP,DT,IFIRST)
    COMMON/FAR/DUM(17),M
    COMMON/STRYIE/STRYT,ERAT
C    6061-T651X ALUMINUM TRUE STRESS-STRAIN PROPERTIES
    IF(EBARP.LE.0.00124) SLOPE=1.7742E6
    IF(EBARP.LE.0.00413.AND.EBARP.GT.0.00124) SLOPE=3.8062E5
    IF(EBARP.LE.0.00991.AND.EBARP.GT.0.00413) SLOPE=2.0761E5
    IF(EBARP.LE.0.0177.AND.EBARP.GT.0.00991) SLOPE=2.439E5
    IF(EBARP.LE.0.0349.AND.EBARP.GT.0.0177) SLOPE=9.884E4
    IF(EBARP.LE.0.0538.AND.EBARP.GT.0.0349) SLOPE=1.0053E5
    IF(EBARP.LE.0.0724.AND.EBARP.GT.0.0538) SLOPE=4.839E4
    IF(EBARP.LE.0.1149.AND.EBARP.GT.0.0724) SLOPE=1.882E4
    IF(EBARP.LE.0.1264.AND.EBARP.GT.0.1149) SLOPE=-5.217E4
    IF(EBARP.GE.0.1264) SLOPE=-1.452E5
    RETURN
    END
    SUBROUTINE UFORMS (S,NRETN,LONG,NDEG,ISTYP,ITI,ISTART,ITIE,

```

```

1LONGSM, ITIEM, LEVEL, NUMNP, DICOS, TRANSM, XORD, NPBT, NBCTRA,
2NCRD, TDICOS, LEVELM, II, LONGTM, DISP, ITYFL)
  DIMENSION S(NDEG, LONGSM), ITI(LONGTM, ITIEM)
  DIMENSION DICOS(NDEG, NDEG), TRANSM(6, 1),
1XORD(NCRD, NUMNP), NPBT(1), TDICOS(NDEG, NDEG),
2DISP(NDEG, LONGTM)
  DO 10 I=1, 12
  DO 11 J=1, 12
    S(I, J)=0.0
11 CONTINUE
10 CONTINUE
  S(1, 1)=.5
  S(1, 7)=.5
  S(2, 2)=.5
  S(2, 8)=.5
  S(3, 3)=.5
  S(3, 9)=.5
  S(4, 4)=.5
  S(4, 10)=.5
  S(5, 5)=.5
  S(5, 11)=.5
  S(6, 6)=.5
  S(6, 12)=.5
  RETURN
  END

```

=EOF=

cat >inpt4.f <<"=EOF="

TITLE IEA STRONGBACK STRUCTURAL ANALYSIS \_UPPER AND LOWER PANELS

TITLE DETERMINATION OF COLLAPSE LOAD

SIZING 400000

ELEMENTS 75

ALL POINTS

LARGE DISP

UPDATE

LOAD COR

MATERIAL, 1,

SHELL SECT, 3,

FOLLOW FOR

END

FIXED DISP

2

COMMENT THE FOLLOWING CARD SETS ARE FROM LOAD ID 100

0.0 0.0

2 3

2 12 21 25 26

0.0 0.0 0.0

1 2 3

10 17 33 41 49

CONNECTIVITY

112 1

1 75 49 47 43 41

2 75 41 43 31 33

3 75 33 31 19 17

4 75 17 19 7 10

5 75 47 45 40 43

6 75 43 40 29 31

7 75 31 29 16 19

8 75 19 16 5 7

9 75 45 38 35 40

10 75 40 35 28 29

11	75	29	28	13	16
12	75	16	13	4	5
13	75	38	26	25	35
14	75	35	25	21	28
15	75	28	21	12	13
16	75	13	12	2	4
17	75	49	48	50	47
18	75	47	50	46	45
19	75	45	46	39	38
20	75	38	39	27	26
21	75	26	27	24	25
22	75	25	24	22	21
23	75	21	22	11	12
24	75	12	11	3	2
25	75	2	3	1	4
26	75	4	1	6	5
27	75	5	6	8	7
28	75	7	8	9	10
29	75	10	9	18	17
30	75	17	18	32	33
31	75	33	32	42	41
32	75	41	42	48	49
49	75	45	46	37	40
50	75	40	37	30	29
51	75	29	30	15	16
52	75	16	15	6	5
53	75	47	50	44	43
54	75	43	44	34	31
55	75	31	34	20	19
56	75	19	20	8	7
57	75	38	39	36	35
58	75	35	36	23	28
59	75	28	23	14	13
60	75	13	14	1	4
61	75	41	42	44	43
62	75	43	44	37	40
63	75	40	37	36	35
64	75	35	36	24	25
65	75	17	18	20	19
66	75	19	20	15	16
67	75	16	15	14	13
68	75	13	14	11	12
69	75	33	32	34	31
70	75	31	34	30	29
71	75	29	30	23	28
72	75	28	23	22	21
73	75	99	97	93	91
74	75	91	93	81	83
75	75	83	81	69	67
76	75	67	69	57	60
77	75	97	95	90	93
78	75	93	90	79	81
79	75	81	79	66	69
80	75	69	66	55	57
81	75	95	88	85	90
82	75	90	85	78	79
83	75	79	78	63	66
84	75	66	63	54	55
85	75	88	76	75	85
86	75	85	75	71	78

87	75	78	71	62	63
88	75	63	62	52	54
89	75	99	98	100	97
90	75	97	95	96	100
91	75	95	88	89	96
92	75	88	89	77	76
93	75	76	77	74	75
94	75	75	71	72	74
95	75	71	62	61	72
96	75	62	52	53	61
97	75	52	54	51	53
98	75	54	55	56	51
99	75	55	57	58	56
100	75	57	60	59	58
101	75	60	67	68	59
102	75	67	83	82	68
103	75	83	91	92	82
104	75	91	99	98	92
121	75	95	90	87	96
122	75	90	79	80	87
123	75	79	66	65	80
124	75	66	55	56	65
125	75	97	93	94	100
126	75	93	81	84	94
127	75	81	69	70	84
128	75	69	57	58	70
129	75	88	85	86	89
130	75	85	78	73	86
131	75	78	63	64	73
132	75	63	54	51	64
133	75	91	93	94	92
134	75	93	90	87	94
135	75	90	85	86	87
136	75	85	75	74	86
137	75	67	69	70	68
138	75	69	66	65	70
139	75	66	63	64	65
140	75	63	62	61	64
141	75	83	81	84	82
142	75	81	79	80	84
143	75	79	78	73	80
144	75	78	71	72	73

COORDINATES

6	100	1	
1	106.8450	78.50000	2.000000
2	142.4600	78.50000	0.0
3	142.4600	78.50000	2.000000
4	106.8450	78.50000	0.0
5	71.23001	78.50000	0.0
6	71.23000	78.50000	2.000000
7	35.61501	78.50000	0.0
8	35.61498	78.50000	2.000000
9	0.0	78.50000	2.000000
10	0.0	78.50000	0.0
11	142.4600	58.87500	2.000000
12	142.4600	58.87500	0.0
13	106.8450	58.87500	0.0
14	106.8450	58.87500	2.000000
15	71.23000	58.87500	2.000000
16	71.23001	58.87500	0.0

17	0.0	58.87500	0.0
18	0.0	58.87500	2.000000
19	35.61501	58.87500	0.0
20	35.61501	58.87500	2.000000
21	142.4600	39.25000	0.0
22	142.4600	39.25000	2.000000
23	106.8450	39.25000	2.000000
24	142.4600	19.62500	2.000000
25	142.4600	19.62500	0.0
26	142.4600	0.0	0.0
27	142.4600	0.0	2.000000
28	106.8450	39.25000	0.0
29	71.23001	39.25000	0.0
30	71.23001	39.25000	2.000000
31	35.61501	39.25000	0.0
32	0.0	39.25000	2.000000
33	0.0	39.25000	0.0
34	35.61500	39.25000	2.000000
35	106.8450	19.62500	0.0
36	106.8450	19.62500	2.000000
37	71.23000	19.62500	2.000000
38	106.8450	0.0	0.0
39	106.8450	0.0	2.000000
40	71.23001	19.62500	0.0
41	0.0	19.62500	0.0
42	0.0	19.62500	2.000000
43	35.61501	19.62500	0.0
44	35.61501	19.62500	2.000000
45	71.23001	0.0	0.0
46	71.23001	0.0	2.000000
47	35.61501	0.0	0.0
48	0.0	0.0	2.000000
49	0.0	0.0	0.0
50	35.61501	0.0	2.000000
51	106.8450	78.50000	2.000000
52	142.4600	78.50000	4.000000
53	142.4600	78.50000	2.000000
54	106.8450	78.50000	4.000000
55	71.23001	78.50000	4.000000
56	71.23000	78.50000	2.000000
57	35.61501	78.50000	4.000000
58	35.61498	78.50000	2.000000
59	0.0	78.50000	2.000000
60	0.0	78.50000	4.000000
61	142.4600	58.87500	2.000000
62	142.4600	58.87500	4.000000
63	106.8450	58.87500	4.000000
64	106.8450	58.87500	2.000000
65	71.23000	58.87500	2.000000
66	71.23001	58.87500	4.000000
67	0.0	58.87500	4.000000
68	0.0	58.87500	2.000000
69	35.61501	58.87500	4.000000
70	35.61501	58.87500	2.000000
71	142.4600	39.25000	4.000000
72	142.4600	39.25000	2.000000
73	106.8450	39.25000	2.000000
74	142.4600	19.62500	2.000000
75	142.4600	19.62500	4.000000
76	142.4600	0.0	4.000000

77	142.4600	0.0	2.000000
78	106.8450	39.25000	4.000000
79	71.23001	39.25000	4.000000
80	71.23001	39.25000	2.000000
81	35.61501	39.25000	4.000000
82	0.0	39.25000	2.000000
83	0.0	39.25000	4.000000
84	35.61500	39.25000	2.000000
85	106.8450	19.62500	4.000000
86	106.8450	19.62500	2.000000
87	71.23000	19.62500	2.000000
88	106.8450	0.0	4.000000
89	106.8450	0.0	2.000000
90	71.23001	19.62500	4.000000
91	0.0	19.62500	4.000000
92	0.0	19.62500	2.000000
93	35.61501	19.62500	4.000000
94	35.61501	19.62500	2.000000
95	71.23001	0.0	4.000000
96	71.23001	0.0	2.000000
97	35.61501	0.0	4.000000
98	0.0	0.0	2.000000
99	0.0	0.0	4.000000
100	35.61501	0.0	2.000000

# GEOMETRY

16  
0.100000  
1 TO 16  
0.150000  
17 TO 20  
0.250000  
21 TO 24  
0.150000  
25 TO 28  
0.250000  
29 TO 32  
0.150000  
49 TO 52  
0.150000  
53 TO 68  
0.150000  
69 TO 72  
0.100000  
73 TO 88  
0.150000  
89 TO 92  
0.250000  
93 TO 96  
0.150000  
97 TO 100  
0.250000  
101 TO 104  
0.150000  
121 TO 124  
0.150000  
125 TO 140  
0.150000  
141 TO 144

# PROPERTY

1,

10.2E6,.33,.098,6.0E-6,70.,35.0E3,,1,

1 TO 144

WORK HARD

-1,,1,

TYING

25

103 3

53

103 11

61

103 22

72

103 24

74

103 27

77

103 1

51

103 14

64

103 23

73

103 36

86

103 39

89

103 6

56

103 15

65

103 30

80

103 37

87

103 46

96

103 8

58

103 20

70

103 34

84

103 44

94

103 50

100

103 9

59

103 18

68

103 32

82

103 42

92

103 48

98

DIST LOADS

11

COMMENT THE FOLLOWING CARD SETS ARE FROM LOAD ID 100

2 -0.630000

73	74	75	76	77	78	79	80	81	82	83	84	85	86	87	C
88															
2	-0.630000														
1	2	3	4	5	6	7	8	9	10	11	12	13	14	15	C
16															
11,-3.434,															
1 TO 16															
31,3.434,															
1 TO 16															
11,-3.434,															
73 TO 88															
31,3.434,															
73 TO 88															
21,14.25,															
1 TO 16															
41,-14.25,															
1 TO 16															
21,14.25,															
73 TO 88															
41,-14.25,															
73 TO 88															
102	-3.2		-1.4		2.5										
1 TO 144															
POINT LOAD															
,-612.0,1538.0,															
2,10,26,49,															
,-1224.0,3076.0,															
4,5,7,12,17,21,25,33,38,41,45,47,															
,-2448.0,6152.0,															
13,16,19,28,29,31,35,40,43,															
,-612.0,-1538.0,															
52,60,76,99,															
,-1224.0,-3076.0,															
54,55,57,62,67,71,75,83,88,91,95,97,															
,-2448.0,-6152.0,															
63,66,69,78,79,81,85,90,93,															
POST															
6,16,17,0,1,19,20,,6,															
11 1 SIGMAXX STRESS COMP.															
12 1 SIGMAYY STRESS COMP.															
13 1 SIGMAXY STRESS COMP.															
14 1 SIGMAYZ STRESS COPM.															
15 1 SIGMAZX STRESS COMP.															
17 1 EQUIV.VON MISES STRESS															
CONTROL															
20,															
UDUMP															
OPTIMIZE,2,															
10,															
PRINT CHOICE															
4,3,2,1,															
1,1,6,6,78,78,88,88,															
29,29,45,45,79,79,															
2,4,															
1,															
SUMMARY															
END OPTION															

## DIST LOADS

```

11
COMMENT THE FOLLOWING CARD SETS ARE FROM LOAD ID 100
  2 -6.30000
 73 74 75 76 77 78 79 80 81 82 83 84 85 86 87
88
  2 -6.30000
  1  2  3  4  5  6  7  8  9 10 11 12 13 14 15
16
11,-34.34,
1 TO 16
31,34.34,
1 TO 16
11,-34.34,
73 TO 88
31,34.34,
73 TO 88
21,142.5,
1 TO 16
41,-142.5,
1 TO 16
21,142.5,
73 TO 88
41,-142.5,
73 TO 88
102 -32.0 -14.0 25.0
1 TO 144
POINT LOAD

```

```

,,, -6120.0,15380.0,
2,10,26,49,
,,, -12240.0,30760.0,
4,5,7,12,17,21,25,33,38,41,45,47,
,,, -24480.0,61520.0,
13,16,19,28,29,31,35,40,43,
,,, 6120.0,-15380.0,
52,60,76,99,
,,, 12240.0,-30760.0,
54,55,57,62,67,71,75,83,88,91,95,97,
,,, 24480.0,-61520.0,
63,66,69,78,79,81,85,90,93,

```

## AUTO INCREMENT

```
0.1,15,10,
```

```
CONTINUE
```

```
=EOF=
```

```
marc i=inpt4.f usub=usub4.f ssd=yes bpatran=stg61 ucft=yes \
```

```
cftopt="-exs -l stdout -o off,nozeroinc" forfiles=" 41 "
```

```
*dispose fort.41 -mUX -t'fn=intpt,t=outpt'
```

```
rm inpt4.f usub4.f
```

```
rm fort.41
```

```
ja
```

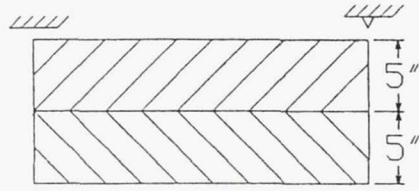
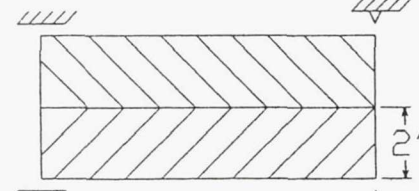
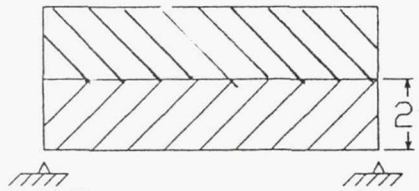
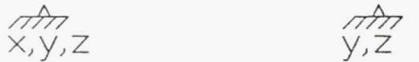
```
ls -al
```

```
ja -t
```

## REFERENCES

1. MARC. Analysis Research Corporation, Revision K.3, July 1988.
2. PATRAN. PDA Engineering, Revision 2.3, July 1988.
3. NASTRAN. The MacNeal-Schwendler Corporation, Version 65C.
4. IDEAS. Structural Dynamics Research Corporation, Version 4, 1988.

TABLE I.—MODELS DESCRIPTION AND RESULTS

Model File.DAT	Boundary support conditions and depth	Type of loading	Pcr collapse load Applied load	Weight of two panels, lb
STG1.*a	B.C.	Uniform pressure + Traction	-----	690.3
STG2A.		Uniform pressure	-----	
STG3.			-----	
STG3B5.	B.C.	Uniform pressure  +  Traction  +  Gravity	966.7	
STG3B2.	B.C.		174.3	473.4
STG4B2.			123.8	328.6
STG4B2P.	B.C.		43.3	
STG5B.	Free		40.3	270.8
STG5BL.			2.593	
STG6L.		(b)	6.4	

<sup>a</sup>Old connectivity.

<sup>b</sup>Includes point moments in addition to the above loading.

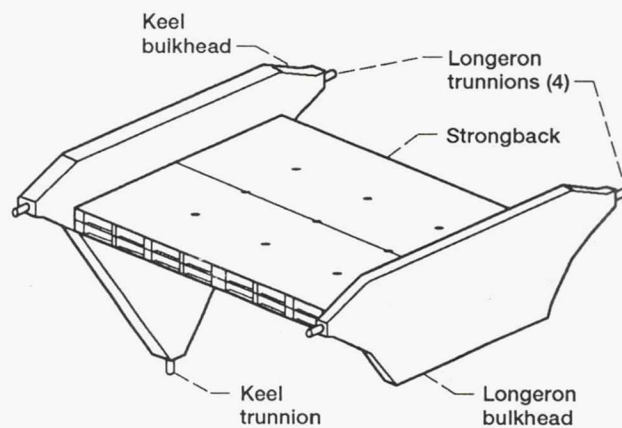


Figure 1.—IEA structural framework.

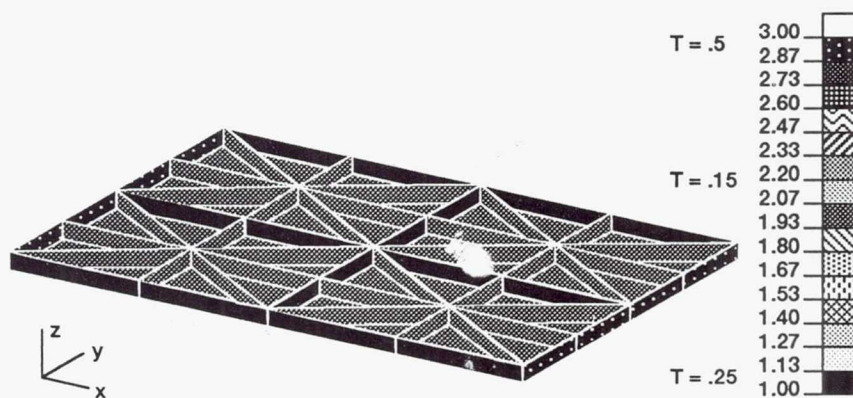
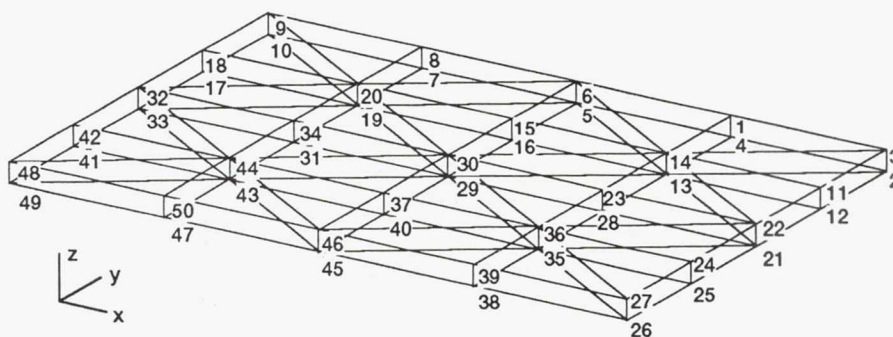


Figure 2.—Geometrical configuration of the strongback panel.



Note:

The lower panel elements connectivity was changed so the node numbers read in a  $\odot$  direction similar to the upper panel. (Origin of z, y, and z axes at node 49.)

Figure 3.—Nodes identification numbers for the lower panel.

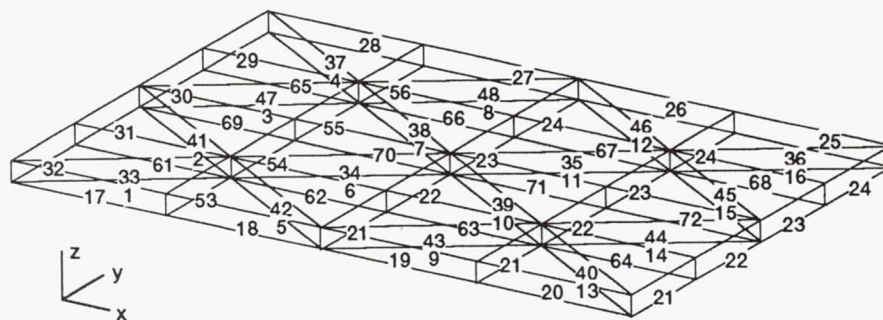


Figure 4.—Elements identification numbers for the lower panel.

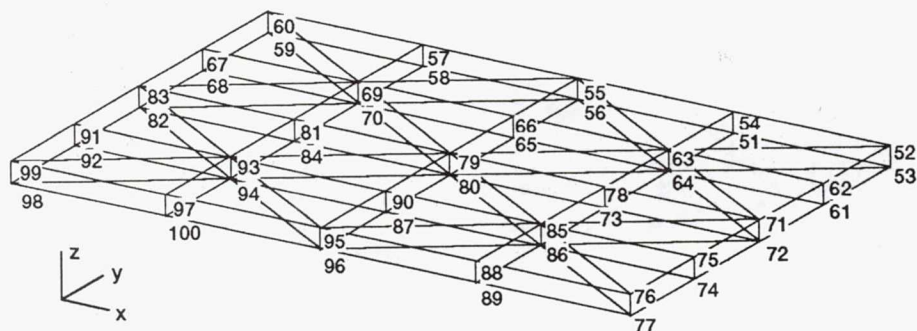


Figure 5.—Nodes identification numbers for the upper panel.

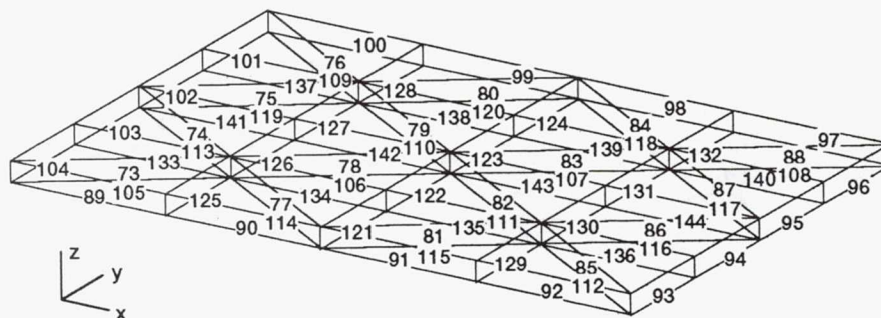


Figure 6.—Elements identification numbers for the upper panel.

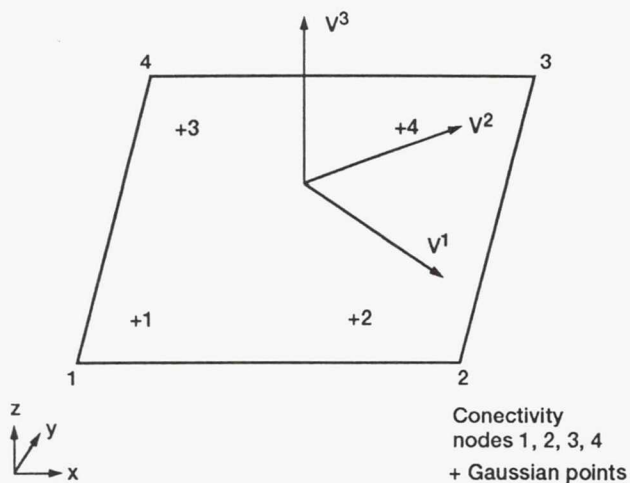


Figure 7.—Nodes connectivity and Gaussian points for element type 75.

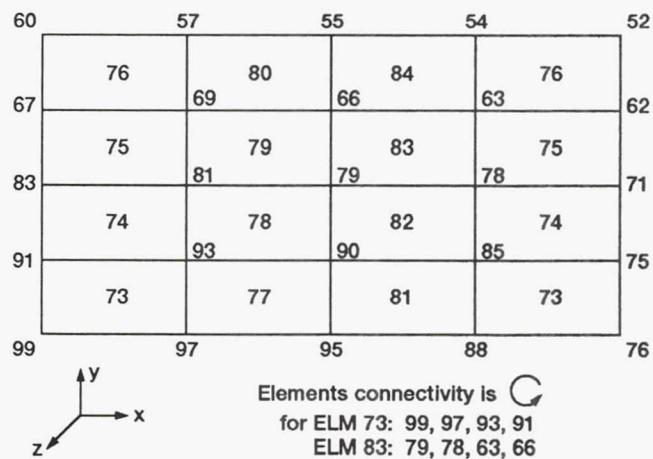


Figure 8.—Elements and nodes identification numbers.

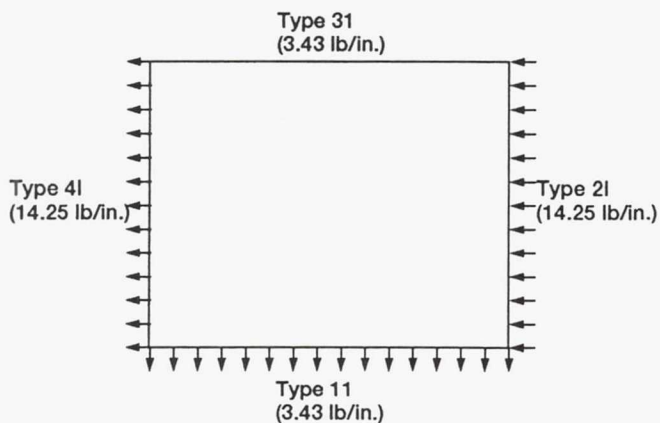


Figure 9.—Traction loads on a typical finite element of the Strongback panels.

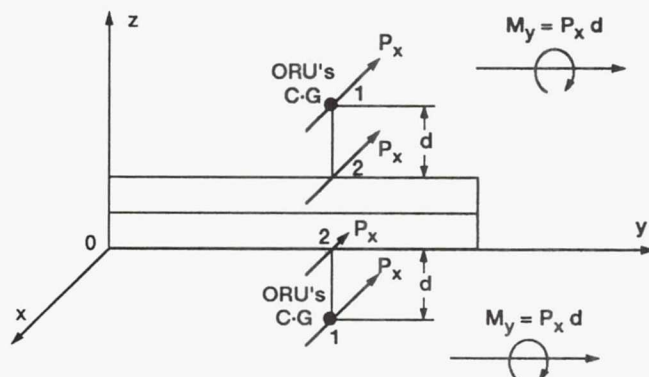


Figure 10.—Transformation of the ORU's loads  $P_x$  to the Strongback panel surface.

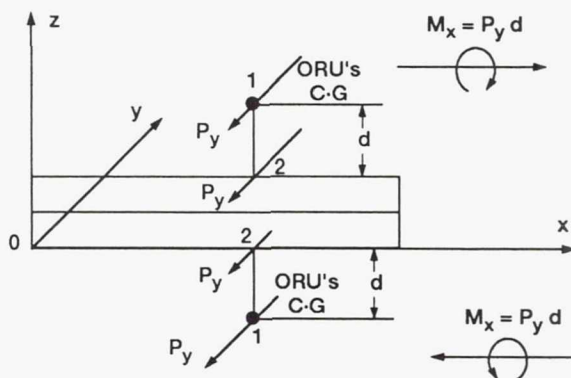


Figure 11.—Transformation of the ORU's loads  $P_y$  to the Strongback panel surface.

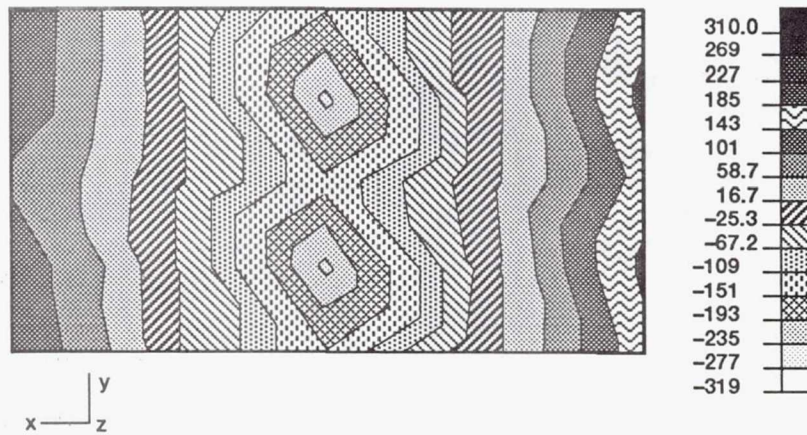


Figure 12.—Sress distribution in the x direction for the upper panel.



Figure 13.—Sress distribution in the y direction for the upper panel.

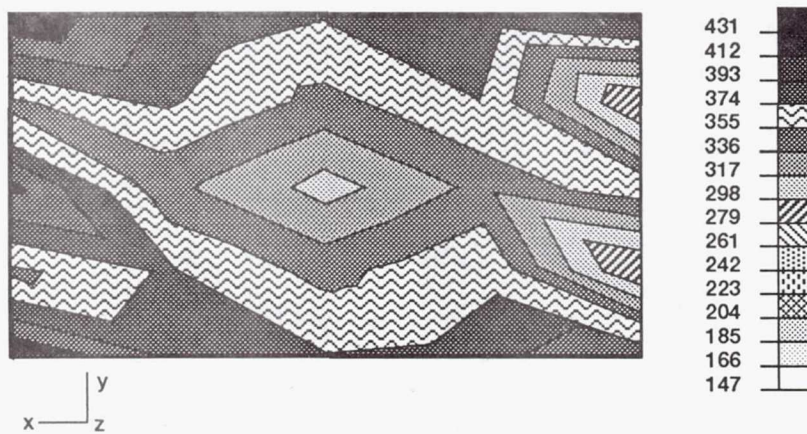


Figure 14.—Nodal Von Mises stress distribution for the upper panel.

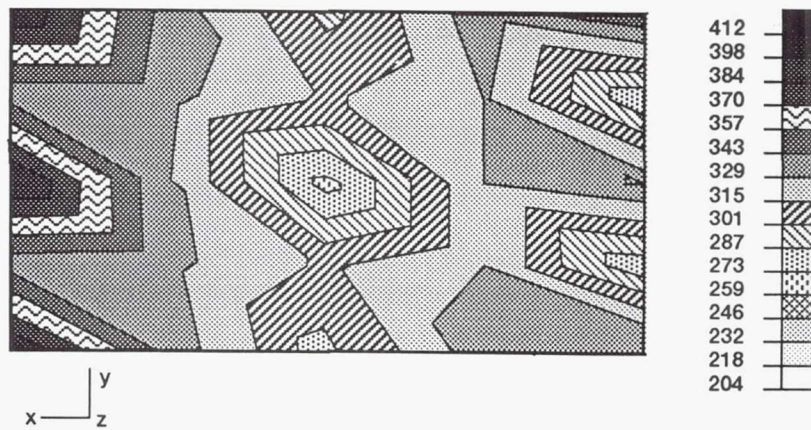


Figure 15.—Element Von Mises stress distribution for the upper panel.



Figure 16.—Stress distribution in the x direction for the lower panel.

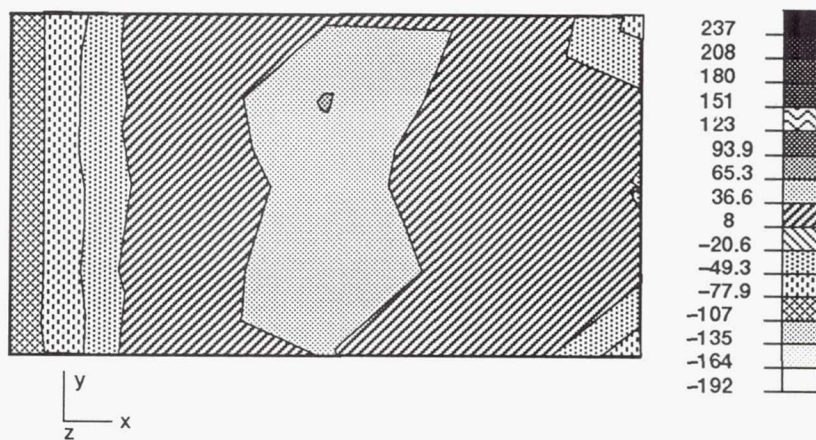


Figure 17.—Stress distribution in the y direction for the lower panel.

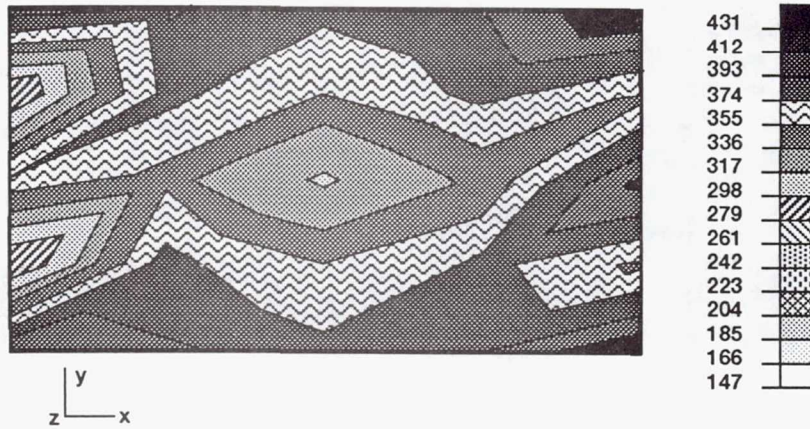


Figure 18.—Nodal Von Mises stress distribution for the lower panel.

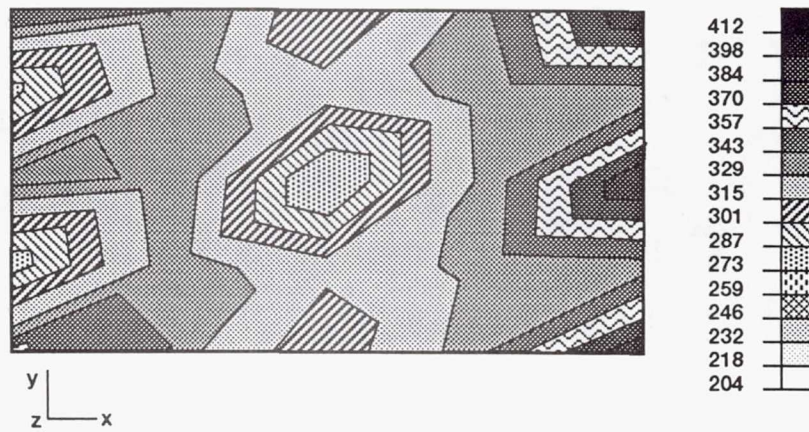


Figure 19.—Element Von Mises stress distribution for the lower panel.



Figure 20.—Stress distribution in the x direction for the upper panel using Nastran.



Figure 21.—Von Mises stress distribution for the upper panel using Nastran.

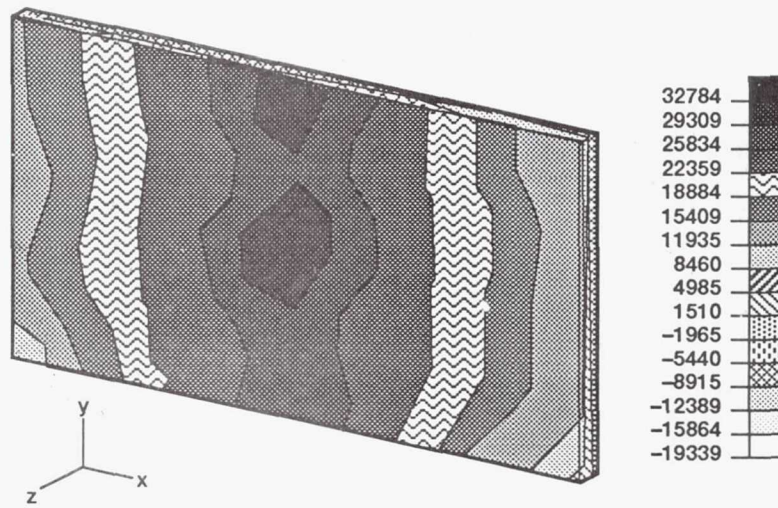


Figure 22.—Maximum principal stress distribution for the upper panel.

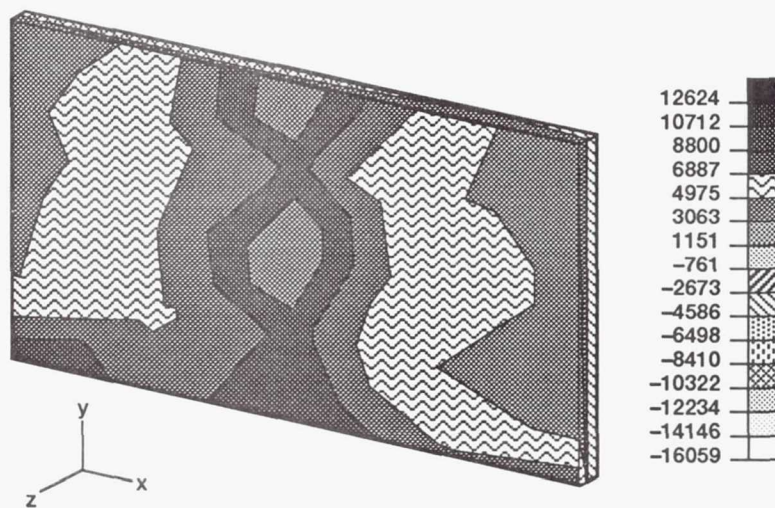


Figure 23.—Minimum principal stress distribution for the upper panel.

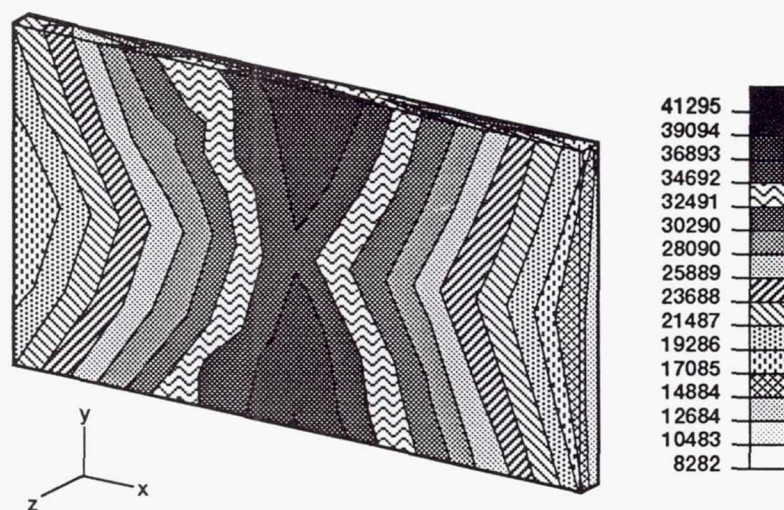


Figure 24.—Element Von Mises stress distribution for the upper panel.

REPORT DOCUMENTATION PAGE			Form Approved OMB No. 0704-0188	
Public reporting burden for this collection of information is estimated to average 1 hour per response, including the time for reviewing instructions, searching existing data sources, gathering and maintaining the data needed, and completing and reviewing the collection of information. Send comments regarding this burden estimate or any other aspect of this collection of information, including suggestions for reducing this burden, to Washington Headquarters Services, Directorate for Information Operations and Reports, 1215 Jefferson Davis Highway, Suite 1204, Arlington, VA 22202-4302, and to the Office of Management and Budget, Paperwork Reduction Project (0704-0188), Washington, DC 20503.				
1. AGENCY USE ONLY (Leave blank)		2. REPORT DATE March 1992		3. REPORT TYPE AND DATES COVERED Technical Memorandum
4. TITLE AND SUBTITLE Collapse Analysis of a Waffle Plate Strongback for Space Station Freedom			5. FUNDING NUMBERS WU-474-46-10	
6. AUTHOR(S) Frank F. Monasa and Joseph M. Roche				
7. PERFORMING ORGANIZATION NAME(S) AND ADDRESS(ES) National Aeronautics and Space Administration Lewis Research Center Cleveland, Ohio 44135-3191			8. PERFORMING ORGANIZATION REPORT NUMBER E-6817	
9. SPONSORING/MONITORING AGENCY NAMES(S) AND ADDRESS(ES) National Aeronautics and Space Administration Washington, D.C. 20546-0001			10. SPONSORING/MONITORING AGENCY REPORT NUMBER NASA TM-105412	
11. SUPPLEMENTARY NOTES Frank F. Monasa, Michigan Technological University, Civil and Environmental Engineering Department, Houghton, Michigan 49931 and Summer Faculty Fellow at NASA Lewis Research Center. Joseph M. Roche, Lewis Research Center. Responsible person, Joseph M. Roche, (216) 433-2575.				
12a. DISTRIBUTION/AVAILABILITY STATEMENT Unclassified - Unlimited Subject Category 39			12b. DISTRIBUTION CODE	
13. ABSTRACT (Maximum 200 words) The purpose of this study was to determine the structural integrity of the Integrated Equipment Assembly (IEA) Strongback of the Space Station Freedom for the launch environment. The strongback structure supports the electrical power system for Space Station Freedom. To achieve minimum launch mass, it is essential that flight structures, such as the strongback, are designed as light as possible. Therefore, the structural analyst must assure the structural integrity of the design. Consequently, a nonlinear structural analysis was conducted to determine the collapse load of the structure and the associated factor of safety against the service loads. Future analysis of flight structures having the general characteristics of the strongback may follow the methodology developed in this report. The report provides a modeling technique for simulating the load conditions and evaluation of the buckling and post-buckling (collapse) loads of the IEA Strongback structure, using the finite element computer code MARC (ref.1). The MARC program was selected for this study due to its capability to perform collapse and nonlinear structural analyses. The strongback structure supports the electrical power system for Space Station Freedom. Two of four strongback panels were modeled and analyzed. This study dealt with the effect of the following factors on the global behavior of the strongback panels: (1) load simplification and simulation; (2) type of support boundary conditions; (3) the possibility of weight reduction of the original structure. For this purpose several models of the two panels of the strongback were considered. The stress level and distribution in the panels for the launch condition, the Eigenvalue critical buckling load and/or the collapse load were determined. Nonlinear structural analysis was required to determine the collapse load. Both geometrical nonlinearity (large deflections) and material nonlinearity were considered. It is shown that a weight reduction of the strongback panels is possible, while maintaining a reasonable factor of safety against the collapse load. This methodology may be useful for future analysis of similar structures.				
14. SUBJECT TERMS Stress analysis; Buckling finite element; Nonlinear			15. NUMBER OF PAGES 36	
			16. PRICE CODE A03	
17. SECURITY CLASSIFICATION OF REPORT Unclassified	18. SECURITY CLASSIFICATION OF THIS PAGE Unclassified	19. SECURITY CLASSIFICATION OF ABSTRACT Unclassified	20. LIMITATION OF ABSTRACT	